

Published in final edited form as:

Cephalalgia. 2012 June ; 32(8): . doi:10.1177/0333102412445622.

Concurrent functional and structural cortical alterations in migraine

Nasim Maleki¹, Lino Becerra^{2,3}, Jennifer Brawn¹, Marcelo Bigal^{4,5}, Rami Burstein⁶, and David Borsook^{2,3}

¹Department of Radiology, Children's Hospital Boston, Harvard Medical School, USA

²Department of Psychiatry, P.A.I.N. Group, Brain Imaging Center, McLean Hospital, Harvard Medical School, USA

³Departments of Psychiatry and Radiology, Massachusetts General Hospital, Harvard Medical School, USA

⁴Merck Investigator Studies Program and Scientific Education Group, Merck Research Laboratories, Merck & Co., Inc., USA

⁵Department of Neurology, Albert Einstein College of Medicine, USA

⁶Department of Anesthesia and Critical Care, Beth Israel Deaconess Medical Center, Harvard Medical School, USA

Abstract

Aim—Various animal and human studies have contributed to the idea of cortical structural–functional alterations in migraine. Defining concurrent cortical alterations may provide specific insights into the unfolding adaptive or maladaptive changes taking place in cortex in migraine.

Methods—From a group of 60 episodic migraineurs, 20 were recruited to the study. Using high-resolution magnetic resonance imaging, structural and functional cortical measures were compared in migraineurs who experienced increased frequency of attacks (HF; 8–14 days/month; $n=10$), to those who experienced less frequent migraine attacks (LF; <2 days/month; $n=10$), and to healthy controls (HC; $n=20$).

Results—Parallel structural and functional differences were found as follows: (i) HF patients showed higher thickness in the area representing the face in the post-central gyrus, which correlated with the observed stronger functional activation, suggesting adaptation to repeated sensory drive; (ii) smaller cortical volume was observed in the cingulate cortex that correlated with lower activation in the HF group; and (iii) similarly significant structural and functional differences (HF>LF) were observed in the insula that may reflect potential alteration in affective processing.

Conclusion—These results suggest differential response patterns in the sensory vs. affective processing regions in the brain that may be an adaptive response to repeated migraine attacks.

© International Headache Society 2012

Corresponding author: David Borsook, P.A.I.N. Group, Brain Imaging Center, McLean Hospital, 115 Mill Street, Belmont, MA 02478, USA, dborsook@partners.org.

Reprints and permissions: sagepub.co.uk/journalsPermissions.nav

Conflict of interests

Dr Bigal is a full-time employee of Merck Inc. He owns stocks and stock options. Other authors have no competing interests to declare.

Keywords

Headache; pain; fMRI; functional connectivity; morphometry; somatosensory cortex; insula; cingulate cortex; temporal pole

Introduction

Cortical changes in migraine have been noted since the earliest descriptions of visual phenomena by Hubert Airy in the 1800s (1), and recent functional studies continue to show alterations in a number of cortical regions in migraine patients (2,3). Alterations in cortical processing include commonly associated phenomena in migraine including evidence of alteration in cortical function in migraineurs. These have included cortical excitability in primary sensory regions (4,5); lack of habituation (6–8), increased sensitivity to sensory input (9,10), noise (phonophobia) (11), and smell (12) in the interictal period (11). These alterations can be explained in part by recent findings in rats that show trigeminovascular inputs from the dura distribute nociceptive information to a number of cortical regions including the primary somatosensory cortices and insular cortices (13). Such data suggest that migraine-induced activation of the trigeminovascular system may through these inputs define correlative neurological symptoms observed in migraine patients.

In parallel with functional imaging studies, anatomical studies of altered brain morphology (gray matter and white matter tracts) have contributed to the idea of structural-functional alterations in migraine. Most of these studies have been performed independently – that is studies reporting either functional or anatomical changes (14–18). The manifestation of altered function may result in altered gray matter changes in migraine patients or vice versa. The significance of defining concurrent differences may provide specific insights into the unfolding adaptive or maladaptive changes taking place in cortical and other brain regions in migraine subjects (19).

In the above the studies mentioned that cortical anatomical differences were evaluated as a function of the health or disease (with or without aura) and were not correlated with functional differences in these regions or networks. An unanswered question is whether functional and anatomical changes in cortical regions are a function of increased frequency of migraine attacks. In a previous report we described significant correlative functional and morphological differences in subcortical regions in a group of matched episodic migraineurs with low and high frequency attacks (19). Here we further investigate the issue in these patients, focusing on possible cortical differences in function and structure by comparing low frequency (LF) vs. high frequency (HF) episodic migraineurs and whether or not functional-anatomical differences are seen in the same cortical regions.

Methods

This study was approved by the McLean Hospital's Institutional Review Board, and it met the criteria of the Helsinki Accord on the Experimentation of Pain in Human Subjects (<http://history.nih.gov/research/downloads/helsinki.pdf>) and approved informed consent forms were obtained from all subjects.

Subjects

Migraine subjects were selected from screening a cohort of 60 migraine sufferers, separated into two groups of 10, each matched for age, age of migraine onset, and medication type. Subjects included in this study met the episodic migraine criteria as defined by the International Classification for Headache (ICHD-2; <http://ihs-classification.org/en/>

02_klassifikation/). Each subject suffered from episodic migraines for at least 3 years and did not experience a migraine 72 hours before the scan and was asymptomatic for 24 hours after the scan. LF subjects experienced 1–2 migraine days per month, while HF patients had 8–14 migraine days per month. Demographic data is presented in Table 1. The migraine attack laterality in the migraine cohorts were as follows: HF (1/10 only right-sided, and the rest experienced migraine attacks on both sides with 5/10 predominantly left-sided, 2/10 predominantly right-sided and 2/10 equally left- and right-sided migraine attacks), and LF (1/10 only right-sided, 1/10 only left-sided and the rest experienced migraine attacks on both sides with 5/10 predominantly right-sided and 3/10 equally left- and right-sided migraine attacks). Each subject's migraine frequency was consistent for the 12 months preceding the imaging scan. Each subject scored 25 on the Beck Depression Inventory II (BDI-II). Patients were not on any other medications, aside from NSAIDs and triptans (see (20)). For comparison, morphometric data of a group of healthy controls (HC, 20 subjects (10 male, 10 female), age 41.8 ± 9.9 years) were acquired and analyzed. The healthy control subjects included in the study met an extensive list of exclusion criteria, specifically no pain or headache disorders (not more than two non-migraine, non-cluster type headaches per year).

Quantitative heat pain threshold testing

Quantitative heat pain threshold testing (QHPTT) was conducted before each scanning session. A 1.6×1.6 cm contact thermode was used to deliver stimuli to the hand (TSA-II, Medoc Advanced Medical Systems, Ramat Yishai, Israel). The same QHPTT paradigm was used for all the subjects to determine their pain threshold (THR). From a baseline of 32°C , the temperature increased at a rate of $1^\circ\text{C}/\text{s}$. The subject was instructed to stop the program once he or she began to feel pain. This was repeated three more times. The THR was the average of at least three measurements. QHPTT was performed on the predominant side of migraine attacks. If there was no predominant side the QHPTT was performed on the left side.

Noxious thermal stimulation

During functional imaging, three blocks of stimulation (30 s baseline/15 s stimulation @ THR+1, not including the ramp periods) were delivered from a baseline temperature of 32°C using the same probe that was used during QHPTT. The end temperature of the delivered stimulation was individualized for each patient based on his or her individually measured pain threshold temperature performed outside the scanner. All patients were consistently feeling pain at that temperature. The rate of temperature change was $4^\circ\text{C}/\text{s}$. The ramps were modeled in defining the explanatory variables (EVs) for fMRI data analysis. A visual analog scale (VAS) system was used for pain and unpleasantness rating by subjects. Similar to QHPTT, thermal stimulation side was the migraine dominant side. If there was no predominant side the stimulation was delivered to the left hand.

Functional and structural imaging

All the imaging data were collected using an 8-channel phased array head coil on a 3 Tesla Siemens Trio scanner (Erlangen, Germany). In this study, structural data was acquired using a 3D MPRAGE pulse sequence (TR/TE/TI=2100/2.74/1100 ms, FA=12°, 128 sagittal slices, res=1.33×1.0×1.0mm³). This sequence produced high-resolution T₁-weighted datasets. Functional data was acquired using a gradient echo (GE) echo planar (EPI) sequence (TE/TR=30/2500 ms, res = 3.5×3.5×3.5mm³, matrix=64×64, 74 volumes, 41 slices).

Data analysis

Structural analysis—Two types of comparisons were performed: cortical thickness comparisons, which were vertex-based comparisons, and volumetric comparisons, which

were based on the volumes obtained for brain structures after segmentation. The following steps were taken using the Freesurfer tools: (i) removal of non-brain tissue using a hybrid watershed/surface deformation procedure; (ii) automated Talairach transformation; (iii) segmentation of the subcortical white matter and deep gray matter volumetric structures; (iv) intensity normalization (21); (v) tessellation of the gray matter/white matter boundary; (vi) automated topology correction (22,23); (vii) surface deformation (24); and (viii) registration of the subjects' brains to a common spherical atlas. Statistical surface maps were generated to assess the cortical thickness differences at each vertex for HF vs. LF migraine patients. Surface data for each subject was smoothed with a 10mm full width at half maximum kernel to improve inter-subject averaging. In order to generate these maps a two-class general linear model was used and age was added to the model as a covariate. The analysis across the entire cortical surface resulted in a statistical surface map that was corrected for multiple comparisons. Clusterwise correction for multiple comparisons was then performed using a Monte Carlo simulation (10,000 iterations). The statistical surface maps were then overlaid on the averaged inflated brain. Masks were created on the average inflated brain for the cortical regions that showed significant (corrected) thickness differences between the LF and HF migraineurs. This mask was transformed to each healthy control subject's cortical space individually in order to measure the cortical thickness in that region.

Statistical analysis of the volumetric data was performed using the SPSS 19.0 statistical package. A univariate analysis of variance for each segmented volume was used to assess the differences between the cohorts (HC, LF and HF). In order to account for the differences in the cranium size an estimate of the total intracranial volume (eTIV) was used as an additional regressor (25) that was estimated based on a statistical relationship between the TIV computed from a manual segmentation and the Talairach transform. These regressors are necessary for this cross-sectional study because the brain structures scale with the general cranium size (25) and also with age (26).

Functional analysis—fMRI analysis was carried out using FMRIB Software Library (FSL) (www.fmrib.ox.ac.uk/fsl), version 4.1.3. Quality assurance (QA) of the data was performed using an in-house developed tool to detect the volumes with spikes or uncorrected motion artifacts. The pre-statistical processing for each subject consisted of skull stripping using a brain extraction tool (BET) with bias field correction and neck removal and motion correction. The volumes were spatially smoothed with a 5mm full-width at half-maximum filter, and a 60 s high-pass temporal filter was applied. First-level fMRI analysis of single subject data was performed using fMRI Expert Analysis Tool (FEAT) Version 5.98. The EVs for thermal stimuli were entered using the recorded temperature traces for each subject. Subjects were spatially normalized to the MNI152 brain for group analysis. Registration was performed using FLIRT (FMRIB's Linear Image Registration Tool) following a two-stage process. First a low-resolution image of the whole brain (acquired with similar imaging parameters to the fMRI acquisition separately) was linearly registered to the high-resolution structural MPRAGE image. Then the MPRAGE image was linearly (affine) registered to the standard image (MNI152 average brain). These two transformations were combined, to transform the low-resolution fMRI images (and the statistical images derived from the first-level analyses) straight into standard space, when applied later, during group analysis. Patients with right-sided migraines had their images flipped along the y-axis to correspond with the majority of the patients with left-sided migraine. The flipping of the fMRI data was performed before the stereotactic normalization. Group activation maps were generated by FEAT FMRIB's Local Analysis of Mixed Effects (FLAME1). Statistical parametric maps were thresholded using a Gaussian mixture model (GMM) technique (27). GMM is a generalized version of false discovery rate (FDR) correction for multiple comparisons in an empirical Bayesian framework. This approach is specially adapted for fMRI thresholding, by being more robust in modeling

violations as compared to traditional FDR by adaptively estimating the form and fraction of ‘null’ from the data (27). In this approach, the ‘activation’ and ‘deactivation’ maps are then thresholded at posterior probability $p > 0.5$. All of the functional results reported in the results section are the results that survived correction for multiple comparisons using GMM.

Functional connectivity analysis—Functional connectivity was measured using a seed correlation based approach (28,29). Regions of interest (ROIs) were defined to test specific hypotheses about the correlation of functional connectivity differences as a function of migraine attacks in the cortical areas that showed morphometric differences between the two cohorts as determined from the structural analysis. All of the seeds were defined anatomically according to the results of the structural analysis. fMRI data processing was carried out using FEAT Version 5.98, as part of FSL (FMRIB’s Software Library, www.fmrib.ox.ac.uk/fsl) (30).

Pre-processing steps were similar to the steps described for functional analysis above. In addition, white matter (WM) and cerebrospinal fluid (CSF) masks were created for each subject and used for confound generation. All time-courses in the brain were orthogonalized with respect to the eigen timecourses of WM and CSF masks (31) and then normalized. The resulting normalized time-courses were entered into a general linear model analysis against the rest of the brain to assess connectivity with the chosen ROI for each subject and then entered into a mixed-effects group analysis (contrast: high frequency – low frequency), FLAME1. The resulting z-statistic maps were thresholded using GMM (27). All of the functional results reported in the results section are the results that survived correction for multiple comparisons using GMM.

Results

Psychophysical/biometric results

There were no significant differences in the patients’ headache intensity: 7.7 ± 2.4 (mean \pm SD) in LF (10 subjects, 40.2 ± 11.3 years) and 7.2 ± 1.8 (mean \pm SD) in HF (10 subjects, 43.9 ± 10.6 years) on a 0–10 subjective scale. However the headache unpleasantness rating was significantly different between the two groups: 8.5 ± 1.8 (mean \pm SD) and 6.7 ± 1.4 (mean \pm SD) in the LF and HF groups, respectively ($p < 0.028$). There were no significant differences between the QHPTT thresholds (LF: $46.06 \pm 4.26^\circ\text{C}$ and HF: $45.89 \pm 2.77^\circ\text{C}$). BDI ratings for subjects were all < 10 , and not significantly different (LF: 2.1 ± 2.5 , HF: 1.9 ± 2.4).

Summary of the imaging findings of this study are presented in Table 2 and will be discussed in detail in the following sections.

In the following the results are organized per structure, i.e. each section will focus on one structure and the functional implication of structural differences in that structure in HF vs. LF migraineurs.

Somatosensory cortex

Contrast analysis of the HF vs. LF migraine group in response to the ‘pain threshold + 1°C ’ stimuli revealed significant differences in the two groups. HF migraine patients showed increased activation in the bilateral post-central gyrus (Figure 1, Table 3). Compared to LF, a cluster of thicker cortex was observed in the HF group in a region in the post-central gyrus of the left hemisphere ($p < 0.008$), which was co-localized with the area that also showed stronger functional activation in the same cohort (in the right hemisphere). Figure 1 shows the thickened area in S1 (HF > LF) overlaid on an average brain. Interestingly, measurement of the cortical thickness in the same region in healthy subjects revealed a significantly

thicker cortex in HC relative to LF patients ($p < 0.01$). A functional connectivity analysis using the MC-corrected post-central gyrus thickened cluster as a seed mask revealed significantly stronger functional connectivity of this post-central area with various areas commonly involved in the processing of pain, as well as in sensory processing areas in HF migraine patients relative to the LF migraine patients such as the anterior cingulate cortex (ACC), posterior insula, thalamus (pulvinar), parahippocampus, hypothalamus, putamen and frontal pole (Figure 1). HF migraine patients also showed lower functional connectivity with the substantia nigra relative to the LF patients.

Cingulate cortex

The HF cohort showed lower activation in the anterior middle cingulate (amc) and posterior middle cingulate (pmc) concurrent with volumetric differences in the cingulate cortex that are shown in Figure 2 and Table 3. There was a significantly lower volume of posterior mid-cingulate in the right hemisphere (rh) ($p < 0.002$), and anterior mid-cingulate (rh) ($p < 0.021$) and anterior cingulate (rh) ($p < 0.03$) in the HF vs. LF migraine patients. Taking into account migraine laterality, a significant reduction of the volume was still observed for the posterior mid-cingulate (rh) ($p < 0.023$), and bilateral anterior mid-cingulate (lh: $p < 0.03$, rh: $p < 0.017$). For this analysis the brains of the subjects who experienced migraine attacks predominantly on the right side were flipped so that they would match those that were mostly experiencing left-sided migraine attacks. Figure 3 shows the analysis results for the cortical volumetric differences in the HF vs. LF migraine patients while accounting for migraine laterality. There were no statistically significant differences between the LF and HC, but HF vs. HC difference was significant ($p < 0.001$ for both amc and pmc). Stronger functional connectivity with the anterior cingulate was observed with frontal pole, temporal pole, inferior temporal gyrus, pulvinar nucleus of the thalamus and parahippocampal gyrus in HF vs. LF migraine patients.

Anterior insula cortex

Significant lower activation in the HF migraine patients relative to the LF migraine patients was observed in contralateral anterior insula and bilateral inferior circular insula (ipsilateral > contralateral) concurrent with structural differences in the same region (Figure 4 and Table 3). There were significant differences in the functional connectivity in HF vs. LF migraine patients during intermittent heat stimuli (pain threshold + 1°C on hand). There was also a significantly stronger functional connectivity with the ACC, putamen, parahippocampal and hippocampal gyrus in HF vs. LF patients. There was a significant reduction of the volume of the inferior circular insula in the left hemisphere (lh) ($p < 0.033$) in HF vs. LF migraine patients. Taking into account the migraine laterality a significant reduction of the volume was still observed for the inferior circular insula (lh) ($p < 0.043$). There were no significant differences between LF and HC but the HF vs. HC differences were significant ($p < 0.05$).

Temporal pole

Stronger activation in the HF group was also observed in the contralateral superior temporal pole, contralateral inferior temporal gyrus and contralateral temporal fusiform (Figure 5). Thicker cortex was observed in the HF group in a region in the inferior temporal gyrus of the right hemisphere ($p < 0.016$). The activation differences in the temporal area were not spatially co-localized with the area that had shown significantly thicker cortex on the MC-corrected cortical thickness contrast map. Measurement of the cortical thickness in the same region in healthy subjects revealed a significantly ($p < 0.002$) thicker cortex in HC relative to LF patients. The thicker region showed stronger functional connectivity with the same

region that was thicker in the post-central gyrus in the HF cohort. Other regions with HF>LF functional connectivity included middle and superior temporal gyrus along with frontal pole.

Discussion

In this study we report on cortical differences in patients who have either low (<2 days/month) or high (8–14 days/month) frequency migraine attacks. There are no clear-cut phases in episodic migraine but probably a continuum. Determination of the migraine frequency was a crucial point as migraine frequency was the characteristic difference between the groups. Our rationale was that migraine presents a spectrum of attacks from no attacks, to few, to many episodic attacks. The frequency of migraine attacks was chosen prospectively. In our cohort, the average age of onset for the LF group was 21.6 ± 3.2 years. The patients had remained LF migraineurs for an average duration of 21.6 ± 4.3 years. The HF migraine patients had comparable average age of onset (24.2 ± 4.4 years) and average duration (21.2 ± 3.3 years) of the disease confirming the fact that the groups only differed in the frequency of migraine attacks.

Because this was a cross-sectional study we were not able to make inferences about the migraine progression. Instead, we hypothesized that comparing the brain differences in two cohorts of migraine patients that are at two extreme ends of the episodic migraine disease spectrum (very mild vs. very severe), but matched otherwise, will provide new insights into the mechanisms of the migraine disease. Doing such a study is very difficult unless you have a large pool of migraine patients from which you can specifically select patients for each of these two extremes. We screened 60 migraine patients for this study. Thus we were able to carefully select and match subjects for this study.

This provided an opportunity to characterize cortical differences in migraine as a function of the increased number of attacks. Our data show that a number of cortical areas are differentially affected in HF vs. LF migraineurs and there are concurrent structural and functional differences in these cortical areas. Thicker cortex was observed in the post-central gyrus in HF vs. LF migraine patients that also showed stronger response to noxious stimulation in the HF group. Other cortical regions (inferior insula, anterior and posterior mid-cingulate) showed a difference in the volume (HF<LF) that was accompanied by concurrent differential response (HF<LF) to noxious stimulation in the same structures in HF patients. Functional connectivity analysis indicated significant differences between the functional connectivity of the structures that had shown structural differences in HF vs. LF migraineurs with the rest of the brain, specifically with the areas involved in pain processing. These cortical differences parallel subcortical differences previously reported for migraine frequency (19) and are consistent with dynamic multisystem brain changes in the migraine condition that may be exacerbated by increased migraine attacks.

Increased activation and cortical thickness

In earlier reports, cortical thickening in migraineurs vs. HC has been reported in the somatosensory cortex of migraineurs vs. HC (14). However, the latter studies did not show a correlation of functional activation in the primary somatosensory cortex as it relates to pain (i.e. evoked activation by noxious stimulation). Here we extend these findings, suggesting that differences in the S1 may relate to the number of migraine attacks and as such may confirm that these differences are a consequence of the disease not the cause of it. Previous reports have noted increased excitability in the somatosensory cortex in migraine (9). In the results presented here, the activation location overlaps with the differences observed in cortical thickness and the region activated correlates to the location on the sensory homunculus represented by the head/face. This localization is verified based on our prior fMRI study on specific localized representations of inputs from the face (32). The

activations observed in our current study are located in the predefined areas determined in our earlier study. Given that the area of cortical thickness difference is restricted and overlaps with the same region, we interpret the differences as a result of increased afferent (nociceptive) drive to the somatosensory cortex as a result of increased attacks (HF>LF). Cortical thickening may relate to increased afferent input to these regions in a manner analogous to activation-dependent thickening following motor training (33) or musical training (34). While the specific mechanism is unclear, these changes may include an increased number or even density of neuronal or glial cells in certain parts of the cortex in a similar manner seen in other brain areas reported in a rat model of pain (35). Consistent with our data, in a related report the somatosensory cortex has been reported to become increasingly sensitized in patients with chronic daily headache, which is a complication of episodic headaches (4).

As noted in the results, functional connectivity with the S1 was noted in other cortical regions including the posterior insula, the anterior and posterior cingulate cortex, the parahippocampal gyrus, the hippocampus and frontal region (see Figure 1). Of these the posterior insula is also involved in nociceptive processing of pain intensity (36). While increased cortical excitability in migraine patients is well documented (9,37), these results indicate specific differences between the HF and LF groups. We interpret this connectivity as related to nociceptive inputs that may interact with other brain regions directly or indirectly through cortical and subcortical pathways involved in nociceptive drive (13). However, the issue is more complex in that some areas showed weaker functional connectivity in the HF group. The connectivity between S1 and the substantia nigra is intriguing because repeated pain may drive diminished dopaminergic systems (involved in reward) (38).

Although activation differences between the HF and LF groups were observed in the temporal pole (TP) and inferior temporal (IT) lobe, no overlap in gray matter morphology was present. However, significant differences in cortical thickness were present in the inferior temporal gyrus but without any functional correlates. We have previously reported fMRI measures of the temporal lobe in migraine patients vs. HCs in the ictal and interictal state (39). Increased activation was observed in the anterior temporal pole and notably, activation in the temporal pole was exacerbated during their ictal vs. interictal phase. In another study (40) we had seen that capsaicin altered noxious stimulus responses in the inferior temporal gyrus. The inferior temporal gyrus is also involved in placebo analgesia (41). Here the differences seem to reflect this sensitized state resulting from migraine in the HF group.

While the HF migraineurs showed statistically significant differences with the HC subjects in all of the regions reported in this study that was not the case for the LF migraineurs. Differences between HC and LF migraineurs were only statistically significant for sensory regions (S1 and IT). In HF migraineurs, cortical thickness in these regions is higher relative to LF migraineurs and in LF migraineurs it is lower relative to HC. We interpret this as an initial damage or 'wear and tear' (42) of these regions with the onset of the disease that then is compensated by an adaptive response of the brain to meet the increased demand for sensory processing, as the frequency of migraine attacks increase. These morphological changes may reflect complex dynamic alterations due to neurochemical changes with repeated migraine attacks (and perhaps in the interictal period) (see (43)). Gray matter changes have been reported to correlate with alterations in synaptic and dendritic changes (35). The underlying notion that migraine alters the brain is consistent with other, more recent reports in the literature (2). On the other hand, alterations in neuronal activity can elicit long-lasting changes in the synaptic strength transmission at excitatory synapses and drugs or disease may modify dendritic spine density and thus synaptic contacts (44).

Decreased activation and cortical thickness

Unlike the somatosensory cortex, other cortical regions showed lower gray matter in HF vs. LF. in the cingulate and the anterior insula. All of these regions are involved in affective processing of pain (45,46). In the case of the cingulate and insula, differences in activation and gray matter volume overlapped, suggesting a function–structure relationship.

The cingulate cortex is activated in most pain studies (47,48). Patients with other kinds of pain disorders such as trigeminal neuropathy demonstrate thinning of cortical regions that include the mid-posterior cingulate (15). In fMRI studies of migraine patients, activation of brain regions in response to noxious stimulation has included the cingulate during the interictal state (49). Here, further insights into how the region may differ in its response to stimuli show differences between the two groups with HF<LF and associated cortical volumetric differences, noted in the mid-cingulate.

The ACC is involved in descending modulation, and activation of the ACC may facilitate spinal nociception via midbrain modulatory systems (50). Activity within the ACC has been reported to be correlated with the subjective experience of pain unpleasantness (51) but not pain intensity. Also specific manipulation of pain unpleasantness produces significant changes in the ACC (52). Our results indicate lower unpleasantness rating along with lower activity of the ACC in the HF group, consistent with the above-described finding. As to the specific differences found in the mid-cingulate that seem to make it more prone to differences observed in the HF group, two findings may bear on the issue. The first is related to plasticity in the nociceptive thalamic- cingulate pathway (53) and the second is the differences in receptor architecture that is observed in the mid-cingulate compared with the anterior and posterior cingulate (54). These differences may relate to “modifications of cingulate synapses (from repeated migraine attacks) appear to regulate afferent signals that may be important to the transition from acute to chronic pain conditions associated with persistent peripheral noxious stimulation” (53).

Activation observed in response to noxious heat in the anterior insula region has been associated with both acute and chronic pain processing (45,46). The region is activated in both ictal and interictal migraine imaging studies (49). The anterior insula is involved in interoception (55), a basis for self-awareness, and may be involved in impending stimulus significance (56). One would expect the regions to be activated with repetitive stimuli, i.e. more migraines. Repetitive stimuli produce repeated challenges so we interpret our result as a potential basis for patients with HF migraine having a blunted response to interoceptive processing of pain, which, from a neurological perspective, may be a consequence of an adaptation process. The awareness of perturbations thus occurs in the pre-ictal migraine and perhaps the interictal migraine state. This view is supported by the connectivity analysis of the insula reported in our results where HF patients show a stronger connectivity with sensory processing regions including the post-central gyrus compared with LF patients. In support of this, behavioral changes in migraine patients include disturbances of body image and physical sensations (57), including alteration of time sense (58); are indicative of alteration of self-perception/ interoception.

The comorbidity among depression disorders (59), anxiety and migraine has been studied (60). For instance there is an increasing risk of depression in patients who have higher frequency headaches as in daily chronic headache (61). The pathways in these disorders overlap extensively with pathways implicated in the generation, perception and regulation of emotions and affective states. As such the decreased cortical gray matter volume in the cingulate cortex and insular cortex that we report here has also been reported in patients with depression (62) and major depressive disorder (63).

In order to determine which regions were modulated relative to the side of stimulation, each functional image was flipped along the y-axis (anterior–posterior axis) before being registered to the standard brain. Thus, we effectively treated voxels in homologous parts of the brain as the same voxel. The use of flipped brains in fMRI analysis is a well-described procedure in clinical pain studies (64–67). A recent fMRI study (68) on the cortical laterality in response to electrical pain stimulation has shown that the somatosensory cortex is activated contralaterally, while the mid/posterior insula, anterior insula and posterior cingulate are activated bilaterally in response to electrical pain stimulation. The same study reports bilateral but right lateralized activation in the anterior cingulate. Therefore for our analysis, flipping of the brain was essential for S1, while flipping should not affect the comparisons for the insula. However, we found a significant difference in the anterior mid-cingulate between cohorts, which was bilateral. In our study the number of subjects that received stimulation on the left side was higher in HF (7 subjects) vs. LF (4 subjects), and the direction of the differences (LF>HF). We therefore performed the analysis without flipping the brains to confirm the difference that we see is not caused by flipping. The results of that analysis are provided in Supplementary Figure 1. As it can be seen the same results were obtained without flipping the brain, with subtle differences in the size of the activated area.

Caveats

Limitations of the present study include the higher use of NSAIDs and triptans in the HF group. However, the similar cortical thickness observed for HC compared with the LF group provides some insights that medications may be a contributory factor. Although both patient cohorts were matched in terms of the history of the medications they had used, in this study we cannot rule out direct triptan-mediated effects on these structures. The issue of the potential influence of triptans as a confounding variable is documented elsewhere (19). In one region (temporal lobe), no overlap of activation and cortical thickness differences were observed: this could in part be explained by a technical shortcoming in the way the functional data was gathered during imaging, where in some of the subjects, that particular area was out of the field of view of imaging and as such that area was excluded during the group level comparison altogether and the final statistical contrast maps did not include that particular region.

Because Blood Oxygenation-Level Dependent (BOLD) response depends heavily on blood volume, one concern could be that the co-localized associations in cortical thickness and BOLD activation could be explained by co-localized differences in blood volume (between the groups) and not function. However some cortical surface-based functional analysis studies that have used cortical thickness at each vertex as a covariate in the analysis have shown that cortical functional activation comparisons remain the same with or without using cortical thickness as a covariate. In addition independence of the spatial distribution of regional brain atrophy and cerebral blood flow has been shown (69). Moreover, our previous studies found no difference in the first peak of the biphasic pain response in the subcortical structures (that also correlated with the measured cognitive responses), suggestive of the fact that the observed difference in BOLD response (that also correlated with the measured cognitive response) was due to the function rather than volume difference (19).

Conclusion

Our results present evidence for co-localized morphometric and functional cortical differences as a probable brain's adaptive response to repeated migraine attacks. The results specifically suggest differential response patterns in the sensory vs. affective processing regions in the brain. It seems that the way the brain deals with increased frequency of migraine attacks is to form some sort of defense mechanism by being less affected

(reduction in size and activity of the affective processing regions) by the increased sensory input while preparing to deal with this increased sensory input by allocating more 'resources' to the job (i.e. by increased cortical thickness and activity).

Supplementary Material

Refer to Web version on PubMed Central for supplementary material.

Acknowledgments

Funding

The work was supported by grants from NIH (K24 NS064050 (NINDS), R01 NS056195 (NINDS), and R01-NS073997 (NINDS) to DB) (data collection) and an Investigator Initiated Grant from Merck and Co. (data analysis).

References

1. Eadie MJ. Hubert Airy, contemporary men of science and the migraine aura. *J R Coll Physicians Edinb.* 2009; 39:263–267. [PubMed: 20608346]
2. May A. New insights into headache: an update on functional and structural imaging findings. *Nat Rev Neurol.* 2009; 5:199–209. [PubMed: 19347025]
3. Geuze E, Westenberg HG, Heinecke A, et al. Thinner prefrontal cortex in veterans with posttraumatic stress disorder. *Neuroimage.* 2008; 41:675–681. [PubMed: 18445532]
4. Coppola G, Curra A, Di Lorenzo C, et al. Abnormal cortical responses to somatosensory stimulation in medication-overuse headache. *BMC Neurol.* 2010; 10:126. [PubMed: 21192822]
5. Chen WT, Lin YY, Fuh JL, et al. Sustained visual cortex hyperexcitability in migraine with persistent visual aura. *Brain.* 2011; 134:2387–2395. [PubMed: 21729907]
6. Ozkul Y, Uckardes A. Median nerve somatosensory evoked potentials in migraine. *Eur J Neurol.* 2002; 9:227–232. [PubMed: 11985630]
7. Schoenen J. Neurophysiological features of the migrainous brain. *Neurol Sci.* 2006; 27(Suppl 2):S77–S81. [PubMed: 16688634]
8. Afra J. Intensity dependence of auditory evoked cortical potentials in migraine. Changes in the peri-ictal period. *Funct Neurol.* 2005; 20:199–200. [PubMed: 16483461]
9. Lang E, Kaltenhauser M, Neundorfer B, et al. Hyperexcitability of the primary somatosensory cortex in migraine – a magnetoencephalographic study. *Brain.* 2004; 127:2459–2469. [PubMed: 15471903]
10. Bouilloche N, Denuelle M, Payoux P, et al. Photophobia in migraine: an interictal PET study of cortical hyperexcitability and its modulation by pain. *J Neurol Neurosurg Psychiatry.* 2010; 81:978–984. [PubMed: 20595138]
11. Ashkenazi A, Mushtaq A, Yang I, et al. Ictal and interictal phonophobia in migraine – a quantitative controlled study. *Cephalalgia.* 2009; 29:1042–1048. [PubMed: 19735532]
12. Demarquay G, Royet JP, Mick G, et al. Olfactory hypersensitivity in migraineurs: a H(2)(15)O-PET study. *Cephalalgia.* 2008; 28:1069–1080. [PubMed: 18727640]
13. Nosedá R, Jakubowski M, Kainz V, et al. Cortical projections of functionally identified thalamic trigeminovascular neurons: implications for migraine headache and its associated symptoms. *J Neurosci.* 2011; 31:14204–14207. [PubMed: 21976505]
14. DaSilva AF, Granziera C, Snyder J, et al. Thickening in the somatosensory cortex of patients with migraine. *Neurology.* 2007; 69:1990–1995. [PubMed: 18025393]
15. DaSilva AF, Granziera C, Tuch DS, et al. Interictal alterations of the trigeminal somatosensory pathway and periaqueductal gray matter in migraine. *Neuroreport.* 2007; 18:301–305. [PubMed: 17435592]
16. Kim JH, Suh SI, Seol HY, et al. Regional grey matter changes in patients with migraine: a voxel-based morphometry study. *Cephalalgia.* 2008; 28:598–604. [PubMed: 18422725]

17. Schmidt-Wilcke T, Ganssbauer S, Neuner T, et al. Subtle grey matter changes between migraine patients and healthy controls. *Cephalalgia*. 2008; 28:1–4. [PubMed: 17986275]
18. Valfre W, Rainero I, Bergui M, et al. Voxel-based morphometry reveals gray matter abnormalities in migraine. *Headache*. 2008; 48:109–117. [PubMed: 18184293]
19. Maleki N, Becerra L, Nutile L, et al. Migraine attacks the Basal Ganglia. *Mol Pain*. 2011; 7:71. [PubMed: 21936901]
20. Bigal ME, Serrano D, Buse D, et al. Acute migraine medications and evolution from episodic to chronic migraine: a longitudinal population-based study. *Headache*. 2008; 48:1157–1168. [PubMed: 18808500]
21. Sled JG, Zijdenbos AP, Evans AC. A nonparametric method for automatic correction of intensity nonuniformity in MRI data. *IEEE Trans Med Imaging*. 1998; 17:87–97. [PubMed: 9617910]
22. Fischl B, Liu A, Dale AM. Automated manifold surgery: constructing geometrically accurate and topologically correct models of the human cerebral cortex. *IEEE Trans Med Imaging*. 2001; 20:70–80. [PubMed: 11293693]
23. Segonne F, Pacheco J, Fischl B. Geometrically accurate topology-correction of cortical surfaces using nonseparating loops. *IEEE Trans Med Imaging*. 2007; 26:518–529. [PubMed: 17427739]
24. Fischl B, Dale AM. Measuring the thickness of the human cerebral cortex from magnetic resonance images. *Proc Natl Acad Sci U S A*. 2000; 97:11050–11055. [PubMed: 10984517]
25. Buckner RL, Head D, Parker J, et al. A unified approach for morphometric and functional data analysis in young, old, and demented adults using automated atlas-based head size normalization: reliability and validation against manual measurement of total intracranial volume. *Neuroimage*. 2004; 23:724–738. [PubMed: 15488422]
26. Goni W, Abe O, Yamasue H, et al. Age-related changes in regional brain volume evaluated by atlas-based method. *Neuroradiology*. 2010; 52:865–873. [PubMed: 20033142]
27. Pendse G, Borsook D, Becerra L. Enhanced false discovery rate using Gaussian mixture models for thresholding fMRI statistical maps. *Neuroimage*. 2009; 47:231–261. [PubMed: 19269334]
28. Fox MD, Snyder AZ, Vincent JL, et al. The human brain is intrinsically organized into dynamic, anticorrelated functional networks. *Proc Natl Acad Sci U S A*. 2005; 102:9673–9678. [PubMed: 15976020]
29. Zhang D, Snyder AZ, Fox MD, et al. Intrinsic functional relations between human cerebral cortex and thalamus. *J Neurophysiol*. 2008; 100:1740–1748. [PubMed: 18701759]
30. Smith SM, Jenkinson M, Woolrich MW, et al. Advances in functional and structural MR image analysis and implementation as FSL. *Neuroimage*. 2004; 23(Suppl 1):S208–S219. [PubMed: 15501092]
31. Golub, G.; Van Loan, CF. *Matrix Computations*. 3. London: The Johns Hopkins University Press; 1996.
32. Moulton EA, Pendse G, Morris S, et al. Segmentally arranged somatotopy within the face representation of human primary somatosensory cortex. *Hum Brain Mapp*. 2009; 30:757–765. [PubMed: 18266215]
33. Anderson BJ, Eckburg PB, Relucio KI. Alterations in the thickness of motor cortical subregions after motor-skill learning and exercise. *Learn Mem*. 2002; 9:1–9. [PubMed: 11917001]
34. Lappe C, Herholz SC, Trainor LJ, et al. Cortical plasticity induced by short-term unimodal and multimodal musical training. *J Neurosci*. 2008; 28:9632–9639. [PubMed: 18815249]
35. Metz AE, Yau HJ, Centeno MV, et al. Morphological and functional reorganization of rat medial prefrontal cortex in neuropathic pain. *Proc Natl Acad Sci U S A*. 2009; 106:2423–2428. [PubMed: 19171885]
36. Coghill RC, Sang CN, Maisog JM, et al. Pain intensity processing within the human brain: a bilateral, distributed mechanism. *J Neurophysiol*. 1999; 82:1934–1943. [PubMed: 10515983]
37. Aurora SK, Barrodale P, Chronicle EP, et al. Cortical inhibition is reduced in chronic and episodic migraine and demonstrates a spectrum of illness. *Headache*. 2005; 45:546–552. [PubMed: 15953273]
38. Scott DJ, Heitzeg MM, Koepp RA, et al. Variations in the human pain stress experience mediated by ventral and dorsal basal ganglia dopamine activity. *J Neurosci*. 2006; 26:10789–10795. [PubMed: 17050717]

39. Moulton EA, Becerra L, Maleki N, et al. Painful heat reveals hyperexcitability of the temporal pole in interictal and ictal migraine states. *Cereb Cortex*. 2011; 21:435–448. [PubMed: 20562317]
40. Moulton EA, Pendse G, Morris S, et al. Capsaicin-induced thermal hyperalgesia and sensitization in the human trigeminal nociceptive pathway: an fMRI study. *Neuroimage*. 2007; 35:1586–1600. [PubMed: 17407825]
41. Nemoto H, Nemoto Y, Toda H, et al. Placebo analgesia: a PET study. *Exp Brain Res*. 2007; 179:655–664. [PubMed: 17287994]
42. Borsook D, Maleki N, Becerra L, et al. Understanding migraine through the lens of maladaptive stress responses: a model disease of allostatic load. *Neuron*. 2012; 73:219–234. [PubMed: 22284178]
43. Lovinger DM. Neurotransmitter roles in synaptic modulation, plasticity and learning in the dorsal striatum. *Neuropharmacology*. 2010; 58:951–961. [PubMed: 20096294]
44. Malenka RC. Synaptic plasticity and AMPA receptor trafficking. *Ann N Y Acad Sci*. 2003; 1003:1–11. [PubMed: 14684431]
45. Brooks JC, Tracey I. The insula: a multidimensional integration site for pain. *Pain*. 2007; 128:1–2. [PubMed: 17254713]
46. Ploner M, Lee MC, Wiech K, et al. Flexible cerebral connectivity patterns subserve contextual modulations of pain. *Cereb Cortex*. 2011; 21:719–726. [PubMed: 20713505]
47. Peyron R, Laurent B, Garcia-Larrea L. Functional imaging of brain responses to pain. A review and meta-analysis. *Neurophysiol Clin*. 2000; 30:263–288. [PubMed: 11126640]
48. Apkarian AV, Bushnell MC, Treede RD, et al. Human brain mechanisms of pain perception and regulation in health and disease. *Eur J Pain*. 2005; 9:463–484. [PubMed: 15979027]
49. Tessitore A, Russo A, Esposito F, et al. Interictal cortical reorganization in episodic migraine without aura: an event-related fMRI study during parametric trigeminal nociceptive stimulation. *Neurol Sci*. 2011; 32(Suppl 1):S165–S167. [PubMed: 21533737]
50. Zhang L, Zhang Y, Zhao ZQ. Anterior cingulate cortex contributes to the descending facilitatory modulation of pain via dorsal reticular nucleus. *Eur J Neurosci*. 2005; 22:1141–1148. [PubMed: 16176356]
51. Rainville P. Brain mechanisms of pain affect and pain modulation. *Curr Opin Neurobiol*. 2002; 12:195–204. [PubMed: 12015237]
52. Hofbauer RK, Rainville P, Duncan GH, et al. Cortical representation of the sensory dimension of pain. *J Neurophysiol*. 2001; 86:402–411. [PubMed: 11431520]
53. Shyu BC, Vogt BA. Short-term synaptic plasticity in the nociceptive thalamic-anterior cingulate pathway. *Mol Pain*. 2009; 5:51. [PubMed: 19732417]
54. Palomero-Gallagher N, Vogt BA, Schleicher A, et al. Receptor architecture of human cingulate cortex: evaluation of the four-region neurobiological model. *Hum Brain Mapp*. 2009; 30:2336–2355. [PubMed: 19034899]
55. Craig AD. How do you feel – now? The anterior insula and human awareness. *Nat Rev Neurosci*. 2009; 10:59–70. [PubMed: 19096369]
56. Lovero KL, Simmons AN, Aron JL, et al. Anterior insular cortex anticipates impending stimulus significance. *Neuroimage*. 2009; 45:976–983. [PubMed: 19280711]
57. Spitzer M. Perceptual disorders in migraine. *Schmerz*. 1988; 2:66–72. [PubMed: 18415291]
58. Golden GS. The Alice in Wonderland syndrome in juvenile migraine. *Pediatrics*. 1979; 63:517–519. [PubMed: 440858]
59. Frediani F, Villani V. Migraine and depression. *Neurol Sci*. 2007; 28(Suppl 2):S161–S165. [PubMed: 17508165]
60. Balaban CD, Jacob RG, Furman JM. Neurologic bases for comorbidity of balance disorders, anxiety disorders and migraine: neurotherapeutic implications. *Expert Rev Neurother*. 2011; 11:379–394. [PubMed: 21375443]
61. Antonaci F, Nappi G, Galli F, et al. Migraine and psychiatric comorbidity: a review of clinical findings. *J Headache Pain*. 2011; 12:115–125. [PubMed: 21210177]

62. Salvatore G, Nugent AC, Lemaitre H, et al. Prefrontal cortical abnormalities in currently depressed versus currently remitted patients with major depressive disorder. *Neuroimage*. 2011; 54:2643–2651. [PubMed: 21073959]
63. Sprengelmeyer R, Steele JD, Mwangi B, et al. The insular cortex and the neuroanatomy of major depression. *J Affect Disord*. 2011; 133:120–127. [PubMed: 21531027]
64. Maihofner C, Handwerker HO, Birklein F. Functional imaging of allodynia in complex regional pain syndrome. *Neurology*. 2006; 66:711–717. [PubMed: 16534108]
65. Schweinhardt P, Glynn C, Brooks J, et al. An fMRI study of cerebral processing of brush-evoked allodynia in neuropathic pain patients. *Neuroimage*. 2006; 32:256–265. [PubMed: 16679031]
66. Moulton EA, Becerra L, Maleki N, et al. Painful heat reveals hyperexcitability of the temporal pole in interictal and ictal migraine states. *Cereb Cortex*. 2011; 21:435–448. [PubMed: 20562317]
67. Pleger B, Ragert P, Schwenkreis P, et al. Patterns of cortical reorganization parallel impaired tactile discrimination and pain intensity in complex regional pain syndrome. *Neuroimage*. 2006; 32:503–510. [PubMed: 16753306]
68. Symonds LL, Gordon NS, Bixby JC, et al. Right-lateralized pain processing in the human cortex: an fMRI study. *J Neurophysiol*. 2006; 95:3823–3830. [PubMed: 16554508]
69. Chen JJ, Rosas HD, Salat DH. Age-associated reductions in cerebral blood flow are independent from regional atrophy. *Neuroimage*. 2011; 55:468–478. [PubMed: 21167947]

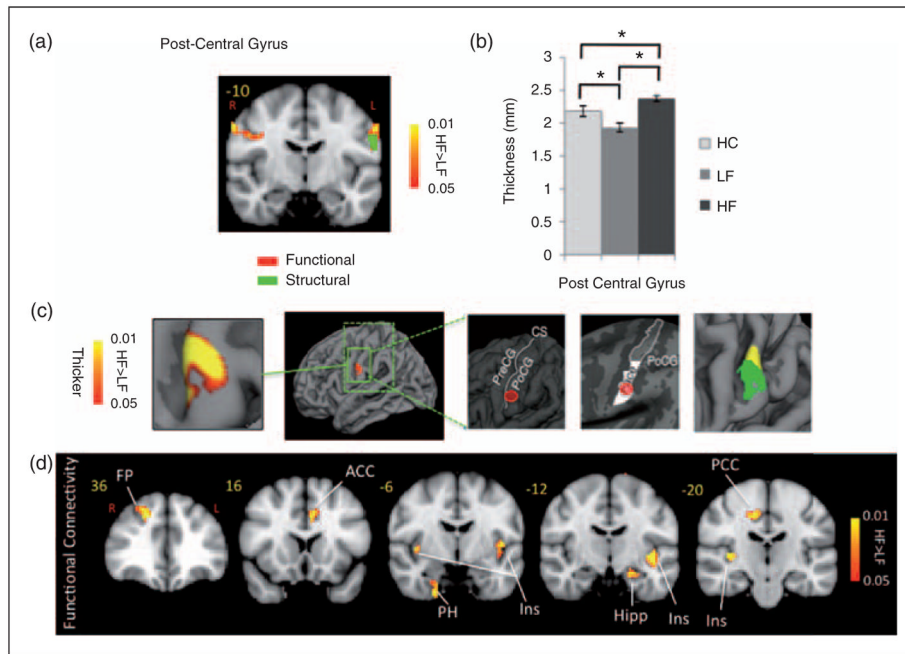


Figure 1.

Post-central gyrus. (a) Functional activation: The figure shows the statistical functional contrast map (HF – LF) in red-yellow color (at GMM-corrected threshold) at the level of the post-central gyri ($y=-10$) along with the region (green) that shows significant co-localized structural difference between the two groups. Bar heights represent the mean value for each volumetric measurement. Error bars represent the 95% confidence interval of the mean. *denotes significance. (b) and (c) Cortical thickness: Comparison of the cortical thickness between the two migraine cohorts and healthy cohort in the post-central gyrus region. In (c) the figure shows the region in the post-central gyrus which is thicker in HF patients and its corresponding statistical map from vertex-wise cortical thickness comparison of (HF – LF, Monte Carlo corrected for multiple comparisons) along with schematic representation of the functional area (face) encompassing this cluster based on the known anatomy. PreCG: pre-central gyrus; POCG: post-central gyrus; CS: central sulcus. The final box shows the overlap between the functional (yellow) and the structural (green) contrasts between the migraine cohorts. (d) Functional connectivity: Functional connectivity contrast of the region in the post-central gyrus with significant structural difference between the two cohorts (i.e. green cluster in (a)) during intermittent heat stimuli (pain threshold+1°C on hand) in HF – LF migraine patients. This region showed significantly stronger functional connectivity with areas involved in pain as well as sensory processing in the HF cohort. ACC: anterior cingulate cortex; PCC: posterior cingulate cortex; Ins: insula; Hipp: hippocampus; PH: parahippocampus; Thal: thalamus; FP: frontal pole.

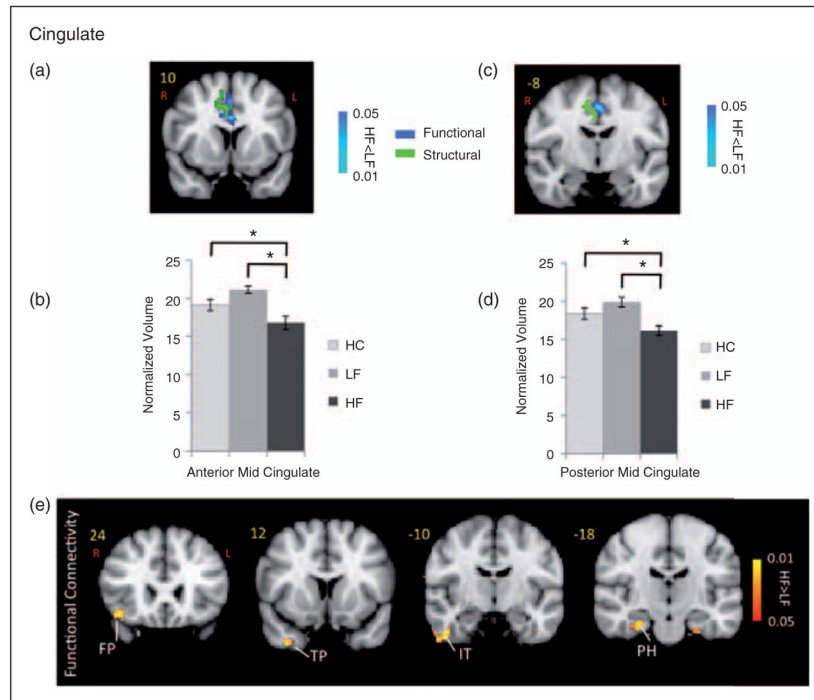


Figure 2. Cingulate gyrus. Figures show overlap between the structural and functional contrasts (HF – LF) in the anterior mid-cingulate ((a) and (b)), and posterior mid-cingulate ((c) and (d)). Statistical functional contrast maps are shown in blue-light blue color (at GMM-corrected threshold) and the regions that showed significant structural differences between the two groups are shown in green. The plots show the significant volumetric differences in the HF vs. LF migraine subjects in the (b) anterior mid-cingulate and (d) posterior mid-cingulate. Healthy control data is also shown for comparison. The volumes have been normalized to the TIV to scale for the brain volume for each subject. Bar heights represent the mean value and the error bars represent the 95% confidence interval of the mean. *denotes significance. (e) Functional connectivity contrast map of ACC during intermittent heat stimuli (pain threshold+ 1°C on hand) in HF migraine patients – LF migraine patients. TP: temporal pole; PH: parahippocampus; FP: frontal pole; IT: inferior temporal.

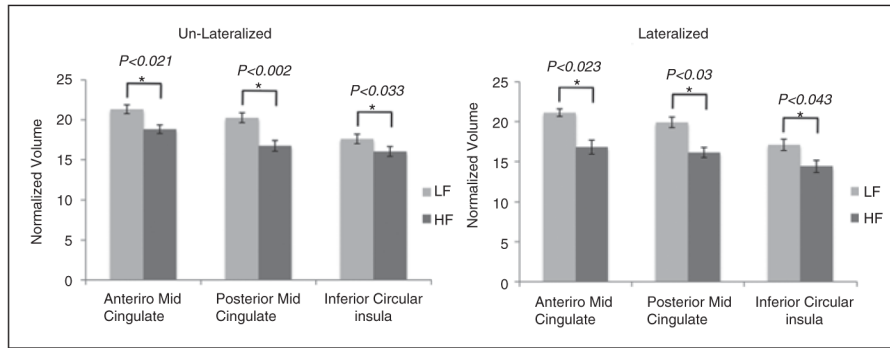


Figure 3.

Laterality. The plots show significant volumetric differences in the HF vs. LF migraine subjects. The ‘Un-Lateralized’ plot shows the comparison results without accounting for the laterality effect (whether attacks happen predominantly on the left side, right side or equally on both sides). The ‘Lateralized’ plot shows the comparison results taking into account the migraine laterality. For this analysis the brains of the subjects who were experiencing migraine attacks predominantly on the right side were flipped so that they would match those that were mostly experiencing left-sided migraine attacks. The volumes have been normalized to the TIV to scale for the brain volume for each subject. Bar heights represent the mean value for each volumetric measurement. Error bars represent the 95% confidence interval of the mean. *denotes a significance level of the corresponding p -value reported. These results indicate that the differences that were found remain the same with accounting for migraine laterality.

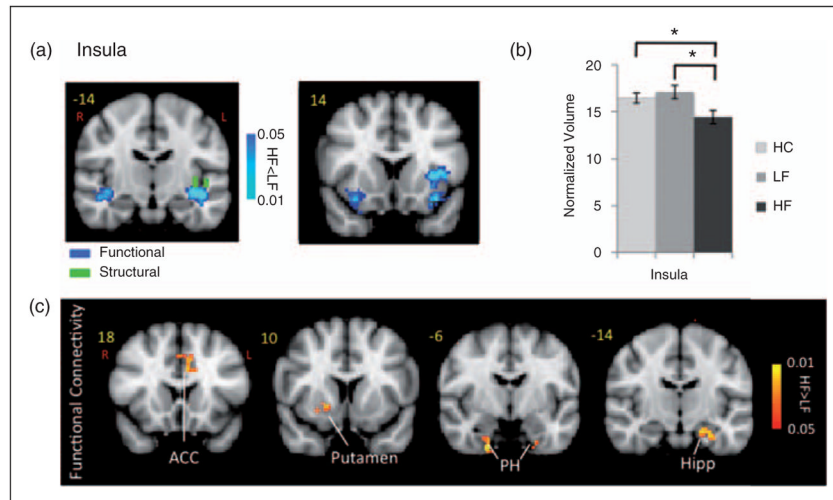


Figure 4.

Insula. (a) Functional activation: Contrast analysis of the HF vs. LF migraine group in response to the pain threshold+1°C stimuli revealed significant differences in the contralateral anterior insula and bilateral inferior circular (stronger contralaterally) which was co-localized with the structural differences (shown in green) in the inferior circular insula. (b) Volumetric differences: The plot shows the significant volumetric difference in the HF vs. LF migraine subjects in the inferior circular insula. Healthy control data is also presented for comparison. The volumes have been normalized to the TIV to scale for the brain volume for each subject. Bar heights represent the mean value and error bars represent the 95% confidence interval of the mean. *denotes significance. (c) Functional connectivity: Functional connectivity contrast maps (HF – LF) for the inferior circular insula region at GMM-corrected threshold. ACC: anterior cingulate cortex; Hipp: hippocampus; PH: parahippocampus.

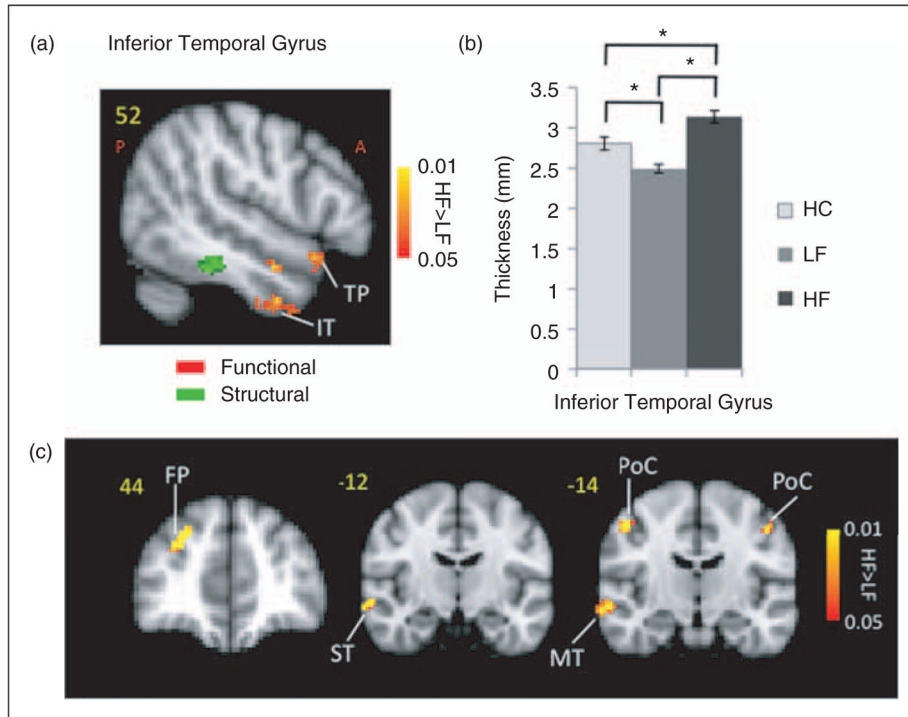


Figure 5.

Temporal lobe. (a) Differences in the temporal lobe activation (red-yellow clusters) in response to noxious (pain threshold+1°C) in HF vs. LF patients. Also shown is a region with the significant structural difference between the two migraine cohorts. (b) The plot shows the significant cortical thickness difference in the HF vs. LF migraine subjects in that region in the inferior temporal lobe. Healthy control data is also presented for comparison. Bar heights represent the mean value and error bars represent the 95% confidence interval of the mean. (c) Functional connectivity contrast maps (HF – LF) for the region with significant structural differences between the two groups in the temporal lobe (green cluster in (a)) at GMM-corrected threshold. ACC: anterior cingulate cortex; ST: superior temporal; FP: frontal pole; MT: middle temporal; PoC: post-central.

Table 1

Patient demographics

Age	Gender	Onset	BDI	Abortive Rx ⁺	Analgesic Rx ⁺	Preventive Rx ⁺	Aura
HF 43.9±3.4	3M, 7F	24.2±4.4	1.9±2.4	80%	80%	20%	1
LF 40.2±3.6	3M, 7F	21.6±3.2	2.1±2.5	80%	50%	10%	1*

Abortive Rx includes rizatriptan, sumatriptan and naratriptan. Analgesic Rx includes ibuprofen, Excedrine migraine and Advil. Preventive Rx includes amitriptyline and verapamil.

* One of the LF patients also occasionally experienced auras.

⁺ This table reports medication history of the patients in terms of the medications that they had used for their headaches, aside from NSAIDS and triptans, during the 12 months prior to the study.

Table 2

Summary of the findings

	Thickness/volume				Functional activity				Functional connectivity	
	HF>LF	LF>HF	HC>LF	HF>HC	HF>LF	LF>HF	HC>HF	HF>HF	HF>LF	LF>HF
SI (post-central gyrus)	+		+	+	+				FP, ACC, PH, Ins, Hipp, PCC	SN
Insula		+				+		+	ACC, Put, PH, Hipp	
Cingulate		+				+		+	FP, TP, IT, PH	
Temporal	+		+	+	+				FP, ST, MT, SI (PoC)	

ACC: anterior cingulate cortex; PCC: posterior cingulate cortex; Ins: insula; Hipp: hippocampus; PH: parahippocampus; FP: frontal pole; TP: temporal pole; IT: inferior temporal; ST: superior temporal; MT: middle temporal; PoC: post-central; SN: substantia nigra.

Table 3

Clusters for painful heat fMRI activation. Contrast of HF vs. LF migraine patients in response to noxious heat (threshold+1°C)

Region	Loc.	Lat.	z-stat	X (mm)	Y (mm)	Z (mm)	Volume (cm ³)
SI	PoC	R	2.1457	-60	-14	36	0.776
		L	1.9735	62	-12	40	0.628
Cingulate	Anterior	R	-1.2573	4	28	24	1.296
	Middle	R	-1.7933	6	24	36	1.12
	Middle	L	-2.3358	0	6	40	0.296
Insula	Middle	L	-1.4795	0	-12	36	1.76
	Anterior	R	-1.4958	42	18	-2	3.032
	Inferior	L	-2.4797	-38	-14	-8	3.648
	Inferior	R	-1.1926	40	-12	-6	2.096

X, Y and Z are coordinates MNI_152_2mm space. Loc (location) and Lat (Laterality).